Accepted Manuscript

Title: Selective Oxidation of Benzyl Alcohol through eco-friendly processes using mesoporous V-MCM-41, Fe-MCM-41 and Co-MCM-41 materials

Authors: Analía L. Cánepa, Verónica R. Elías, Virginia M. Vaschetti, Ema V. Sabre, Griselda A. Eimer, Sandra G. Casuscelli

Selective Oxidation of Benzyl Alcohol through eco-friendly processes using mesoporous V-MCM-41, Fe-MCM-41 and Co-MCM-41 materials

Analía L. Cánepa, Verónica R. Elías, Virginia M. Vaschetti, Ema V. Sabre Griselda A. Eimer, Sandra G. Casuscelli[*]

Centro de Investigación y Tecnología Química, UTN-CONICET, Facultad Regional Córdoba, Maestro López esq. Cruz Roja Argentina, S/N, X5016ZAA, Córdoba, Argentina.

- CORRESPONDING AUTHOR FOOTNOTE. Dra. Sandra G. Casuscelli, e-mail: scasuscelli@frc.utn.edu.ar, CITeQ, UTN-CONICET Tel./Fax: 54-351-4690585.

Graphical abstract
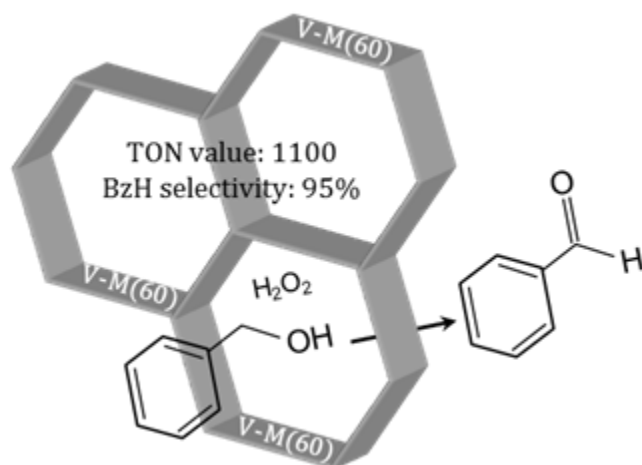
Highlights

- *MCM-41 materials modified with V, Fe or Co were synthetized by hydrothermal method*
- *The activity of V-M(60), Fe-M(60) and Co-M(60)were tested in benzyl alcohol oxidation*

1

- *The V-M(60) exhibited better catalytic activity: TON (1100) and selectivity to BzH of 95%*
- *The V-M(60) did not show loss of activity and selectivity after several cycles*

Abstract

MCM-41 nanostructured materials modified with Vanadium, Iron and Cobalt were synthesized by a hydrothermal method. The catalysts were characterized by XRD, UV-Vis-DR, ICP-OES and N_2 adsorption. All the catalysts showed good structural order and high specific areas; however the lowest value in these parameters, corresponding to the Co-M(60) sample, could be due to the higher presence of oxide species determined by UV-Vis-DR. These mesoporous metalosilicates were evaluated in the liquid phase oxidation of benzyl alcohol (BzOH) to benzaldehyde (BzH) using H_2O_2 as oxidant. Results showed that V-M(60) had better catalytic performance than Fe-M(60) and Co-M(60) exhibiting high TON (1100 mol/mol V), selectivity to BzH (95 %) and 31.7 % yield at 7 h under optimized reaction conditions. The main reason for the enhanced catalytic performance was attributed to the well dispersion of vanadium species in the framework which could be considered as the active sites for the benzyl alcohol oxidation reaction. At the same time, the catalyst could be recovered and effectively reused during three cycles without a significant loss in its activity and selectivity.

1. Introduction

The selective oxidation of alcohols into the corresponding carbonyl compounds plays a vital role in the organic synthesis since the corresponding aldehyde; ketone or carboxylic derivatives serve as important and versatile intermediates for the synthesis of

2

various chemicals, vitamins, drugs and fragrances [1-10]. Benzaldehyde (BzH) is a typical product of benzyl alcohol (BzOH) oxidation and a chief raw material in the synthesis of other organic compounds, ranging from pharmaceuticals to plastic additives. It is also widely used as an intermediate for the manufacturing of odorants, drugs, dyestuffs and agrochemicals [11-13]. It is traditionally produced by hydrolysis of benzal chloride and by oxidation of toluene [14,15]. However, BzH produced from hydrolysis of benzal chloride has often some unfavorable aspects such as containing traces of chlorine impurities and generating copious waste. The oxidation of toluene is usually carried out in organic solvents which are environmentally undesirable [16]. The most common methods of oxidation use stoichiometric amounts of inorganic oxygen donors such as manganese or chromium for this transformation [17-20]. However, these oxidants are corrosive, expensive, they have low atom efficiency and they generate big amounts of heavy-metal waste [21,22]. The increasing demand for environment-conscious chemical processes and the need of chlorine-free BzH have impelled many researchers to investigate green technologies [23-36]. Several studies have been reported on the catalytic oxidation of BzOH to BzH with different catalysts and oxidants. Supported noble metal catalysts such as Pd/SiO_2 [37], Au/SBA-15 [38], Au-Pd/TiO_2 [39] and Ag/SBA-15 [40] have been used in the aerobic oxidation of BzOH to BzH. Unfortunately, high costs generally limit the large scale use of noble metal based catalysts. In addition, copper and gold nanoparticules supported on γ-Al_2O_3 [41], CoMgAl hydrotalcites [42] and vanadium phosphate [43] were also evaluated as catalysts using tert-butyl hydro peroxide. On the other hand, hydrogen peroxide is an environmentally friendly oxidant for liquid phase oxidations because it provides high content of active oxygen species and water is the only byproduct. Many efforts have been devoted to the selective oxidation of benzyl alcohol by H_2O_2 employing different

3

solid catalysts. Cang et al. have achieved high turnover numbers TON (125.8) using imidaziolium-FeCl$_3$ ionic liquid immobilized onto SBA-15 and H$_2$O$_2$ as oxidant in a H$_2$O$_2$/BzOH molar ratio of 4/1 [44]. Jia et al. reported a conversion of benzyl alcohol and a selectivity to benzaldehyde about 53 % and 86 % respectively on alkali treated ZSM-5 with H$_2$O$_2$ [45]. Epiclhlorydrin-modified Fe$_3$O$_4$ microspheres were employed by Xiago et al. obtaining a conversion of benzyl alcohol of 34.7 % and 93 % of selectivity to benzaldehyde [46].

MCM-41 is a member of the M41S family with particular characteristics such as large pore volume, uniform distribution in pore size and high specific surface area. These characteristics make them interesting materials to be employed specially in oxidation reactions that involve large molecules and required high selectivity. Nevertheless, some modification of the pure siliceous material (Si-M) is necessary due to its lack of catalytic activity. Recent research has indicated that Si-M modified with transition metals could be potentially used as an effective heterogeneous catalyst with custom properties in eco-compatible processes. Particularly, it is of great interest to develop catalysts based on available transition metals commonly used by living beings such as iron, cobalt, molybdenum [47] which are not environmental hazardous. The incorporation of metallic ions such as Ti, V, Fe and Co in the network structure of molecular sieves has showed good results for the liquid phase oxidation of organic molecules. Thus, Ti-MCM-41 has been used to catalyze the oxidation of various organic compounds e.g. allylic alcohols, olefins and terpenes with H$_2$O$_2$ [48-50]. V- MCM-41 has also been well studied in the oxidation of cyclic compounds, olefins and bulkier olefins with H$_2$O$_2$ as oxidant [51-54]. In addition, Fe-MCM-41 and Co-MCM-41 have been shown to be active in the oxidation of styrene, cyclohexene and ethyl benzene [55-57]. However, few studies have reported the use of mesoporous materials modified with

transition metals in the selective oxidation of benzyl alcohol to benzaldehyde.

Trakarnpruk reported a benzyl alcohol conversion of about 78 % and a selectivity to

benzaldehyde of 67 % using Mn- and Co-substituted polyoxotungstates on MCM-41

and a molar ratio H_2O_2/BzOH 3/1 in a Parr reactor [58].

In this work, a series of MCM modified with Co, V and Fe have been prepared by a

hydrothermal method. These materials were then characterized and used to catalyze the

oxidation of BzOH employing H_2O_2 as oxidant. The effect of the concentration of H_2O_2

on the catalytic performance has been investigated. Special attention was paid to the

reaction product selectivity as a function of the concentration of H_2O_2, and the catalytic

behavior was related to the metal species observed by UV–Vis-DR.

2. Experimental

2.1. Catalyst synthesis

The mesoporous metalosilicates were prepared by hydrothermal synthesis using

cetyltrimethylammonium bromide (CTAB) dissolved in ethanol as a template,

tetraethoxisilane (TEOS) as a Si source and $VO(SO_4).H_2O$, $Fe(NO_3)_3.9H_2O$ or

$Co(NO_3)_2.6H_2O$ as metal sources. Tetraethylammonium hydroxide 20 wt % aqueous

solution (TEAOH) was added in order to adjust the gel pH to 11. The catalysts were

synthesized from gel of molar composition Si/M = 60 (where M indicates V, Fe or Co),

TEAOH/Si = 0.30, CTAB/Si = 0.30, H_2O/ Si = 60. In a typical synthesis, TEOS and the

metal source were stirred for 30 min, the CTAB solution and 70 % of the TEAOH were

added and the stirring continued for 3 h. Finally, the remaining TEAOH and the water

were further added dropwise to the milky solution which was then heated at 80 ºC for

30 min to remove the ethanol used in the solution and produced in the hydrolysis of

TEOS. This gel was transferred into a Teflon-lined stainless-steel autoclave and kept in

5

an oven at 100 ºC for 4 days under autogenous pressure. Mesoporous silicate (Si-M) was prepared by the same method but without the addition of a metal source [59]. The final solids were then filtered, washed with distilled water and dried at 60 ºC overnight. To remove the template, the samples were heated (heating rate of 2 ºC.min^{-1}) under N_2 flow up to 500 ºC maintaining this temperature for 6 h and subsequently calcined at 500 ºC under air flow for 6 h. The obtained materials were named M-M(60) where the first M indicates the metal (V, Fe or Co) and 60 is the Si/M ratio used in the synthesis gel.

2.2. Physicochemical characterization

The metal content in the obtained solids was determined by Inductively Coupled Plasma Optical Emission Spectroscopy (ICP-OES) after digestion of the solids using a VISTA-MPX CCP Simultaneous ICP-OES Varian. XRD patterns were obtained in a PANalytical X´Pert PRO diffractometer. The UV-Vis Diffuse Reflectance (UV-Vis DR) spectra were obtained in a Jasco V650 spectrometer. The specific surfaces were measured using a Micromeritics Pulse Chemisorb 2700. Samples were previously dried using a N_2 flux for 3 h at 350 ºC. The specific surface was determined by the Brunauer-Emmett-Teller (BET) method. A Micromeritic ChemiSorb 2720 was used when Temperature-Programmed Reduction (TPR) experiments were necessary. For this, the samples were heated from 298 to 900 ºC at a rate of 10 ºC.min^{-1} in the presence of 5 % H_2/N_2 gas mixture (20 mL/min STP), and the reduction reaction was monitored by the H_2 consumption with a built-in thermal conductivity detector (TCD).

2.3. Catalytic activity

Benzyl alcohol (BzOH) oxidation reactions with H_2O_2 were carried out in a glass reactor with a magnetic stirrer and a reflux condenser, immersed in a thermally controlled bath at 70 ºC for 7 h. In a typical reaction, benzyl alcohol (Fluka > 95 %) (9.11 mmol), was stirred with hydrogen peroxide (H_2O_2, Riedel de Haën, 35 wt. % in water) (2.28 mmol), using acetonitrile (AcN, Sintorgan, 99.5 %) (91.15 mmol) as solvent and M-M(60) as catalyst (100 mg). Reaction progress was followed taking samples at different times by a lateral tabulation without opening the reactor. Liquid samples were immediately filtered and analyzed by gas chromatography equipped with FID detector (HP-1 capillary column) and identified by comparison with known standards. The percentage of each component in the reaction mixture was calculated by using the method of area normalization employing response factors. The BzOH conversion was defined as the ratio of converted species to the initial moles, Equation (1). Taking into account that BzOH was found in excess in comparison to H_2O_2, the BzOH conversion was also calculated as a percentage of the maximum possible conversion (mol % of max.), that is the maximum amount of the oxygenated products that could be obtained if all H_2O_2 was consumed, Equation (2). The total conversion of H_2O_2 was measured by iodometric titration, while selectivity to products, yield and turnover numbers (TON) were calculated according to Equations (3), (4) and (5):

$$\text{Conversion BzOH}\left(\%\right) = \frac{\text{total moles of product}}{\text{initial moles BzOH}} \times 100 \qquad (1)$$

$$\text{Conversion BzOH}\left(\text{mol\% of max.}\right) = \frac{\text{total moles of product}}{\text{initial moles BzOH} \times \dfrac{\text{initial moles H}_2\text{O}_2}{\text{initial moles BzOH}}} \times 100 \quad (2)$$

7

$$\text{Selectivity}_i\,(\%)=\frac{\text{moles of product}_i}{\text{total moles of product}}\times 100 \tag{3}$$

$$\text{Yield}_i\,(\%)=\text{Conversion BzOH}\,(\%)\times \text{Selectivity}_i \tag{4}$$

$$\text{TON}=\frac{\text{moles of BzOH converted}}{\text{moles of metal in the catalyst}}\times 100 \tag{5}$$

3. Results and discussion

3.1. Catalyst Characterization

Physicochemical parameters and XRD patterns of the pure Si-M and metal modified M-M(60) samples by direct incorporation of the metal source in the synthesis gel are shown in Table 1 and Figure 1. As it can be observed, for pure Si-M, the sample exhibited a strong peak at $2\theta = 2.4°$ with a wide and weak reflection between 3.5 and 5.5 which could correspond to the diffraction of the planes (100) and to the overlap of the planes (110) and (200), respectively. These signals are characteristic of M41S type mesoporous materials. In regards to the metals-modified materials, V-M(60) showed the best structure because its spectrum is similar to the spectrum of Si-M. The materials modified with Fe and Co also showed MCM-41 mesoporous structure although the pore order was slightly lower as it is inferred by the widening of the first peak and the lack of the two reflections at a higher angle.

Also, the highest unit cell parameter value (a_0) for the Co-M(60) sample is in concordance to the lowest structural ordering observed by XRD. In contrast, the smallest and similar a_0 values for the other samples (Si-M, V-M(60) y Fe-M(60)) would

8

correspond to the higher degree of structure ordering attributed to the formation of Si–O–Si bridges and additional network cross linking [60-62]. This ordering could not be achieved when Co was present in the synthesis gel, probably due to the synthesis method used which is not suitable for this metal.

It should be noted that, for all solids, no peaks corresponding to the presence of oxide species were detected in the XRD patterns at high angle (2 theta above 20°), not shown here. This fact allows us to infer that if these species exist they would be amorphous or have a size lower than the limit detection of the technique (6 nm).

The presence of different metal species in the mesoporous synthesized materials was analyzed by UV-Vis DR spectroscopy, Figure 2. According to a previous report [54], the spectrum of the V-M(60) solid have three characteristic absorption bands: Two of them at 250 and 290 nm corresponding to isolated V ions tetrahedrally coordinated with oxygen ligands present inside the walls and in the wall surfaces, respectively [63]. The third band at 320 nm is associated with V ions in octahedral coordination from a probably incipient polymerization of the metal species. As it could be observed, a higher proportion of V is present as tetrahedrally coordinated isolated V ions incorporated into the structure.

On the other hand, it is known that Fe modified silicates show three absorption regions around 200-310 nm, 310-450 nm and 450-650 nm. The first is usually associated with the d_{π}-p_{π} charge transfer between Fe and O indicating that the isolated Fe^{3+} cations are linked to O resulting in their incorporation on the matrix surface [64]. The absorption regions at a higher wavelength give evidences of the presence of $(FeO)_n$ clusters formed in extra red positions and/or small nanoparticles of Fe_2O_3. The absorption in the last region (450-650 nm) is usually associated to the presence of Fe oxide nanoparticles of bigger size. The spectrum of the Fe-M(60) sample shows an intense absorption at 270

nm indicating that the applied synthesis method results in a high incorporation of Fe in the structure as isolated ions. It is noteworthy that this material shows no absorption at wavelengths higher than 450 nm indicating the absence of large iron oxide nanoparticles [65,66]. This is in concordance to that observed by high angle XRD evidencing the refining effect of the hydrothermal treatment on the Fe species formed in the structure [67].

UV-Vis DR spectrum of Co-M(60) showed the presence of bands between 200-300 nm and 300-400 nm assigned to the charge transfer of tetrahedral coordinated Co^{2+} or Co^{3+} ions and O, respectively. The small absorption above 400 nm is associated with octahedral Co^{2+} species, probably present in CoO clusters. The band between 600 nm and 800 nm was attributed to the presence of Co_3O_4 nanoparticles. It is important to note that these mentioned species would be of smaller size than those obtained by other methods of post synthesis, evidencing also the refining effect of the applied hydrothermal treatment [65]. Finally, pure Si-M did not exhibit any absorption in the range of 200–800 nm. [68].

Table 1 shows the chemical composition and structural properties of the synthesized catalysts. As it can be observed, V-M(60) and Fe-M(60) showed a specific surface higher than 900 $m^2.g^{-1}$, which is typical of mesoporous materials. On the other hand, this parameter for Co-M(60) was considerably reduced probably due to the greater incorporation of metal as extra red species.

3.2. Catalytic activity

The synthesized catalysts were tested in the oxidation reaction of BzOH employing H_2O_2 as oxidant and acetonitrile as solvent. The BzOH conversion as a percentage of the maximum possible conversion (mol % of max.) and the selectivity to BzH over V-

M(60), Fe-M(60) and Co-M(60) at different reaction time are shown in Figure 3. At the beginning of reaction with V-M(60), the conversion of BzOH increases fast during the first hour of reaction and then remained almost stable. For Fe-M(60), a progressive increase with the reaction time was observed reaching a maximal conversion of 53% after 7 h, while Co-M(60) showed a very low BzOH conversion. These results can be related to the oxidant consumption. For V-M(60) a conversion of H_2O_2 of 85% was reached at the first hour of reaction which is due to the consume of H_2O_2 by oxidation of BzOH and self-decomposition. Then, the low concentration of the remaining oxidant limited the reaction, that is why the conversion of BzOH remained almost stable after this reaction time. The conversion of H_2O_2 for the reaction with Fe-M (60) reached 36 % in the first hour of reaction increasing progressively with the reaction time, thus the oxidant was still available to oxidize BzOH. Co-M(60) showed high consumption of H_2O_2 (93 % at 1h) and low conversion of BzOH (3.5 % of max.). Thus, this catalyst showed a great tendency to decompose H_2O_2. This results combined with the material characterization by UV–vis-DR described above (Figure 2) allow us to suggest that the CoO clusters and the Co_3O_4 nano-particles could accelerate the decomposition of H_2O_2, giving account for the high consumption of H_2O_2 and the low conversion of BzOH. On the other hand, the selectivity to BzH over V-M(60) and Co-M(60) was maximal, reaching a value of 100 % even after 7 h of reaction, while on Fe-M(60) it reached a value of 90.5 %. This slight decrease in selectivity to BzH for the Fe-M(60) is due to the further oxidation of BzH to benzoic acid (BzA) and benzyl benzoate (BzB), which appeared as reaction by-products (Scheme 1) with a selectivity of 6.0 and 3.5 % respectively.

11

The catalytic performance of the synthesized catalysts, employing a molar ratio substrate/oxidant of 4/1 and 7 h of reaction is summarized in Table 2. As it can be seen, BzH was the main product with a yield of 7 % and 12 % for V-M(60) and Fe-M(60) respectively. According to literature, the intrinsic catalytic activity of different metal catalysts can best be compared when expressed by their turnover number (TON), defined as converted moles per active site [69]. In this paper, these values were calculated on the premise that all the metal present in the synthesized material could be considered as an active site. Thus, TON values obtained for all synthesized catalysts are shown in Table 2. These results show that V-M(60) performance is much better than that of Fe-M(60) and Co-M(60). Thus, the high TON value of the V-M(60) sample could be giving account for the high efficiency of V cations dispersed in the network, which would be the active sites for this reaction. Meanwhile, the low value observed for Co-M(60) could be explained considering the high proportion of metal that was forming species of oxides less dispersed in the siliceous structure, which diminished its catalytic performance as it was discussed in more detail above. Anyway, the values of conversion and selectivity achieved with Fe-M(60) are suitable for the oxidation of BzOH.

In addition, blank experiments, without any catalyst or with metal-free silica were carried out under the same reaction conditions. The reaction did not proceed in the absence of the catalyst and the BzOH conversion on pure silica Si-M was very low (< 0.2 %). Therefore, the enhanced conversion observed over M-M(60) clearly indicates that the incorporation of an isolated metal cation on the mesoporous structure should play an important role for the present reaction. Taking into account the results, we have selected the catalysts modified with Fe and with V to continue the study.

12

It is known that the catalytic properties of Fe modified solids could be studied by reducibility, which was determined by H_2-TPR [70]. The TPR curve of the Fe-M(60) sample is shown in Figure 4. As it was already reported [67] for solids with low Fe content, the two TPR peaks at 415 and 530 ºC can be related to $Fe_2O_3 \rightarrow Fe_3O_4$ and $Fe_3O_4 \rightarrow FeO$ processes, respectively. The hydrogen consumption at temperatures higher than 700 ºC is related to framework Fe^{3+} species of difficult reducibility, giving account for the shielding effect of the MCM-41 structure which results in high stability for these species. Then, from the TPR analysis it could be observed that the direct incorporation synthesis method with 4 days of hydrothermal treatment provokes that Fe^{3+} species are reduced only to Fe^{2+} [65]. Taking into account this TPR analysis, Fe-M(60) was submitted to a reduction treatment in order to clarify the influence of the different Fe species on the catalytic activity. Then, the sample was placed in a quartz reactor, heated at a rate of 10 K.min^{-1} under H_2 flow up to 600 ºC and kept at this temperature for 6 h. This temperature was chosen in order to reach the reduction of the Fe species. The resulting material was named: Fe-M(60)R, where R indicates that the sample was reduced. The UV-Vis DR spectra of the Fe modified solid before and after applying the reduction treatment are shown in Figure 5. When the spectrum of the Fe-M(60)R sample was compared with that of the Fe-M(60) sample, a reduction in the light absorption ability was observed; in fact, a clear decrease between 200 and 300 nm and no absorption over 350 nm was shown. According to the TPR analysis, the UV-Vis-DR analysis shows that Fe^{3+} species present in small oxide nanoparticles or clusters have been reduced and the absorption at short wavelength for the reduced sample is probably due to the presence of hardly reducible dispersed and linked Fe^{3+} species. Then, it could be concluded that H_2 treatment causes the reduction of oxidized Fe species in bigger proportion. Then, the Fe-M(60)R sample was evaluated as catalyst in the oxidation

13

reaction of BzOH. A low TON value of around 23 and a conversion of H_2O_2 of 97 % were observed at 7 h of reaction. Comparing the H_2O_2 conversion achieved for Fe-M(60)R and Fe-M(60), higher values were observed for the reduced sample. These results can be related to the presence of Fe^{2+} on the surface of the solid after the reduction process, as observed by TPR. These species would be involved in the decomposition of H_2O_2, being its reduction by Fe^{2+} the initial step as shown in Equation 6. Then, the peroxide radical, generated by the reaction of the $HO^{\bullet}$ with H_2O_2, transfers one electron to Fe^{3+} (Equation 7 and 8). These results clearly indicate that the presence of Fe^{3+} on the Fe-M(60) surface plays an important role in the BzOH oxidation.

$$Fe^{2+} + H_2O_2 \rightarrow Fe^{3+} + OH^{\bullet} + OH^{-} \tag{6}$$

$$OH^{\bullet} + H_2O_2 \rightarrow HOO^{\bullet} + H_2O \tag{7}$$

$$HOO^{\bullet} + Fe^{3+} \rightarrow Fe^{2+} + H^{+} + O_2 \tag{8}$$

Although the value of TON reached with Fe-M(60) was low, the conversion and selectivity achieved were important, that is why it is justifiable to continue the study of this material in the future. Meanwhile, taking into account the high TON and excellent selectivity with the V-M(60) catalyst, the present study was continued in order to improve the results of the oxidation reaction. Thus, the oxidation of BzOH was investigated for the BzOH/H_2O_2 mole ratio of 2/1 and 1/1 for a reaction period of 7 h. The catalytic performance of BzOH oxidation as a function of reaction time and H_2O_2 amount is depicted in Figure 6 (a-c). It can be seen from Figure 6 (a) and (b) that the TON values increased more pronouncedly for the ratio 4/1 and 2/1 in the first hour of reaction and then remained constant, which is due to consumption of H_2O_2 by oxidation of BzOH and its self-decomposition. Meanwhile, for the relation 1/1, Figure 6 (c) shows

14

that TON values increased with reaction progress since H_2O_2 was available for the oxidation in the reaction medium. On the other hand, selectivity to BzH after 7 h of reaction decreased from 100 % to 65 % when the ratio changed from 4/1 to 1/1. The decrease in BzH selectivity was due to further oxidation of BzH to benzoic acid caused by the high concentration of H_2O_2. Besides, BzH also induced the formation of a small amount of benzyl benzoate as a by-product of reaction. In spite of the decrease in selectivity observed when increasing the amount of oxidant, the yield to BzH increased from 7, for a molar ratio of 4/1, to values of 12 % and 22 % for molar ratios 2/1 and 1/1 respectively.

Therefore, in order to improve both the TON values and the BzH yield, we have considered appropriate to restore the initial ratio $BzOH/H_2O_2$ 4/1 in the reaction medium by additional peroxide aggregates (limiting reactive) [71]. Thus, the following methodology was applied: a) one H_2O_2 aggregate after 1 h and b) three H_2O_2 aggregates at 1 h intervals. Under the first condition (a), the TON reached a value similar to that obtained with a $BzOH/H_2O_2$ molar ratio 2/1 (~ 500) and a slightly better BzH yield of 14.3 % at 7 h of reaction. It is interesting to note that BzH was the only product formed, so at low H_2O_2 concentrations it was possible to maintain the selectivity of BzH at 100 %. With three additional H_2O_2 aggregates, it was also possible to preserve the BzH from subsequent oxidations, reaching a maximum yield of 31.7 % with a TON of 1100 and a selectivity of 95 % at 7 h of reaction. It is important to note the improvement achieved in the BzH selectivity compared to the 65 % obtained when using a 1/1 ratio at the start of the reaction. This results show that the oxidation of BzOH to BzH is highly selective when the H_2O_2 concentration remains low.

In addition, we have performed a recycling study of the V-M(60) at a $BzOH/H_2O_2$ molar ratio of 4/1 with further addition of H_2O_2 at 1h of reaction. At the end of each

reaction, V-M(60) was separated from the reaction mixture by filtration, thoroughly washed with acetonitrile and calcined at 500 ºC overnight. Then it was reused as catalyst in a new reaction under the same conditions. From Figure 7 it can be seen that TON values remained between 480 and 490 for the three cycles performed. At the same time, selectivity to BzH stayed almost constant with values between 97 and 100 %. These results show that the catalyst could be recovered and effectively reused during three cycles without a significant loss in its activity and selectivity, as long as the H_2O_2 concentration remains low.

4. Conclusions

Nanostructured silicates MCM-41 modified by the direct incorporation method with V, Fe or Co were successfully synthesized. All solids showed good structural order, which was evidenced by the XRD patterns and the high specific areas characteristic of this kind of mesostructured materials. The lower surface measured for the Co modified sample could be a consequence of the segregated Co oxide species of bigger size, whose presence was inferred by the major absorption of this sample at a longer wavelength in the UV-vis spectra. The solids modified with Fe and V showed good activity for the benzyl alcohol oxidation. Thus, applying a H_2 reduction treatment on the Fe-M(60) sample, it could be concluded that Fe^{3+} on surface plays an important role for the BzOH oxidation. Then, with the aim of optimizing the catalytic performance, different $BzOH/H_2O_2$ mole ratios were evaluated for the V-M(60) sample. A BzH yield of 12 %, a selectivity of 100 % and high TON (500) were obtained for one additional H_2O_2 aggregate after 1 h of reaction. Meanwhile, with three additional H_2O_2 aggregates at 1 h intervals, it was also possible to reach a maximum yield of 31.7 % with a TON of 1100 and a selectivity of 95 % at 7 h of reaction. It is important to note the improvement

16

achieved in the BzH selectivity compared to the 65 % obtained when using a 1/1 ratio at the start of the reaction. Finally, this catalyst could be used during three catalytic cycles without loss in its activity and selectivity.

4. Acknowledgments

17

5. References

[1] R. A. Sheldon, J. K. Kochi, Metal-Catalyzed Oxidations of Organic Compounds, first ed., Academic Press, New York, 1981.

[2] M. Hudlicky, Oxidations in Organic Chemistry, first ed., American Chemical Society, Washington DC, 1990.

[3] P. S. N. Rao, K. T. V. Rao, P. S. Sai Prasad, N. Lingaiah, Chin. J. Catal. 32 (2011) 1719-1726.

[4] S. R. Ali, P. Chandra, M. Latwal, S. K. Jain, V. K. Bansal, S. P. Singh, Chin. J. Catal. 32 (2011) 1844-1849.

[5] C. Zhou, Y. Liu, Chin. J. Catal. 31 (2010) 656-660.

[6] G. Chatel, C. Monnier, N. Kardos, C. Voiron, B. Andrioletti, M. Draye, Appl. Catal. A 478 (2014) 157-164.

[7] V. Palermo, P. I. Villabrille, P. G. Vazquez, C. V. Caceres, P. Tundo, G. P. Romanelli, J. Chem. Sci. 125 (2013) 1375-1383.

[8] A. Shaabani, E. Farhangi, A. Rahmati, Monatsh. Chem. 139 (2008) 905-908.

[9] M. M. Mojtahedi, M. R. Saidi, M. Bolourtchian, J. S. Shirzi, Monatsh. Chem. 132 (2001) 655-658.

[10] M. A. Zolfigol, M. Hajjami, A. Ghorbani-Choghamarani, J. Iran. Chem. Soc. 9 (2012) 13-18.

[11] J. Zhu, P. C. Wang, M. Lu, Appl. Catal. A. 477 (2014) 125-131.

[12] A. R. Bekhradnia, F. Zahir, S. Arshadi, Monatsh. Chem. 139 (2008) 521-523.

[13] S. Rautiainen, O. Simakova, H. Guo, A. R. Leino, K. Kordás, D. Murzin, M. Leskelä, T. Repo, Appl. Catal. A 485 (2014) 202-206.

[14] D. V. McGrath, R. H. Grubbs, J. W. Ziller, J. Am. Chem. Soc. 113 (1991) 3611–3613.

[15] D. A. Knight, T. L. Schull, Synth. Commun. 33 (2003) 827–831.

[16] V. R. Choudhary, P. A. Chaudhari, V. S. Narkhede, Catal. Commun. 4 (2003) 171–175.

[17] B. Bahramian, V. Mirkhani, M. Moghadam, A. H. Amin, Appl. Catal. A. 315 (2006) 52-57.

[18] J. D. Lou, C. L. Gao, L. Li, Z. G. Fang, Monatsh. Chem. 137 (2006) 1071-1074.

[19] S. Tangestaninejad, M. Moghadam, V. Mirkhani, I. Mohammadpoor-Baltork, N. Hoseini, J. Iran. Chem. Soc. 7 (2010) 663-672.

[20] A. Ghorbani-Choghamarani, G. Azadi, J. Iran. Chem. Soc. 8 (2011) 1082-1090.

[21] T. Mallat, A. Baiker, Chem. Rev. 104 (2004) 3037–3058.

[22] L. I. Simándi, Dioxygen Activation and Homogeneous Catalytic Oxidation: Proceedings of the Fourth International Symposium on Dioxygen Activation and Homogeneous Catalytic Oxidation, first ed., Elsevier Science Ltd, 1991.

[23] M. G. Buonomenna, E. Drioli, Appl. Catal. B: Environ. 79 (2008) 35–42.

[24] M. L. Guo, H. Z. Li, Green Chem. 9 (2007) 421–423.

[25] V. R. Choudhary, R. Jha, P. Jana, Green Chem. 9 (2007) 267–272.

[26] H. Han, S. Zhang, H. Hou, Y. Fan, Y. Zhu, Eur. J. Inorg. Chem. (2006) 1594–1600.

[27] V. R. Choudhary, D. K. Dumbre, V. S. Narkhede, S. K. Jana, Catal. Lett. 86 (2003) 229–233.

[28] G. Wu, X. Wang, J. Li, N. Zhao, W. Wei, Y. Sun, Catal. Today 131 (2008) 402–407.

[29] V. R. Choudhary, D. K. Dumbre, B. S. Uphade, V. S. Narkhede, J. Mol. Catal. A: Chem. 215 (2004) 129–135.

[30] S. Endud, K. L. Wong, Micropor. Mesopor. Mater. 101 (2007) 256–263.

[31] X. Wang, G. Wu, J. Li, N. Zhao, W. Wei, Y. Sun, Catal. Lett. 119 (2007) 87–94.

[32] X. Pan, N. Zhang, X. Fu, Y. J. Xu, Appl. Catal. A. 453 (2013) 181-187.

[33] A. R. Hajipour, H. Karimi, Chin. J. Catal. 35 (2014) 1529-1533.

[34] A. R. Hajipour, H. Karimi, A. Koohi, Chin. J. Catal. 36 (2015) 1109-1116.

[35] H. Zhang, L. Fu, H. Zhong, Chin. J. Catal. 34 (2013) 1848-1854.

[36] A. Shaabani, S. Keshipour, M. Hamidzad, M. Seyyedhamzeh, J. Chem. Sci. 126 (2014) 111-115.

[37] L. Li, J. Zhao, J. Yang, T. Fu, N. Xue, L. Peng, X. Guo, W. Ding, RSC Adv. 5 (2015) 4766-4769.

[38] A. Kumar, B. Sreedhar, K. V. R. Chary, J. Nanosci. Nanotechnol. 15 (2015) 1714-1724.

[39] T. Jiang, C. Jia, L. Zhang, S. He, Y. Sang, H. Li, Y. Li, X. Xu, H. Liu, Nanoscale 7 (2015) 209-220.

[40] L. Ma, l. Jia, X. Guo, L. Xiang, Chin. J. Catal. 35 (2014) 108-119.

[41] M. J. Ndolomingo, R. Meijboom, Appl. Surf. Sci. 398 (2017) 19–32.

[42] W. Zhou, J. Liu, J. Pan, F. Sun, M. He, Q. Chen, Catal. Com. 69 (2015) 1-4.

[43] G. Behera, K. Parida, Appl. Catal. A. 413-414 (2012) 245-253.

[44] R. Cang, B. Lu, X. Li, R. Niu, J. Zhao, Q. Cai, Chem. Eng. Sci. 137 (2015) 268-275.

[45] A. Jia, L. Lou, C. Zhang, Y. Zhang, S. Liu, J. Mol. Catal. A-Chem. 306 (2009) 123–129

[46] S. Xiao, C. Zhang, R. Chen, F. Chen, New J. Chem. 39 (2015) 4924–4932.

[47] S. Enthaler, K. Junge, M. Beller, Angew. Chem. Int. Ed 47 (2008) 3317-3321.

[48] A. Wróblewska, A. Fajdek, J. Wajzberg, E. Milchert, J. Hazard. Mater. 170 (2009) 405–410.

[49] G. A. Eimer, S. G. Casuscelli, C. M. Chanquía, V. Elías, M. E. Crivello, E. R. Herrero, Catal. Today 133–135 (2008) 639–646.

[50] S. G. Casuscelli, G. A. Eimer, A. Cánepa, A. C. Heredia, C. E. Poncio, M. E. Crivello, C. F. Perez, A. Aguilar, E. R. Herrero, Catal. Today 133–135 (2008) 678–683.

[51] K. Wu, B. Li, C. Han, J. Liu, Appl. Catal. A 479 (2014) 70–75.

[52] S. Shylesh, A. P. Singh, J. Catal. 233 (2005) 359–371.

[53] P. Selvam, S. E. Dapurkar, J. Catal. 229 (2005) 64–71.

[54] A. L. Cánepa, C. M. Chanquía, V. M. Vaschetti, G. A. Eimer, S. G. Casuscelli, J. Mol. Catal. A-Chem. 404 (2015) 65–73.

[55] Y. Wang, Q. Zhang, T. Shishido, K. Takehira, J. Catal. 209 (2002) 186–196.

[56] V. R. Elías, M. I. Oliva, S. E. Urreta, S. P. Silvetti, K. Sapag, A. M. Mudarra Navarro, S. G. Casuscelli, G. A. Eimer, Appl. Catal. A. 381 (2010) 92–100.

[57] S. S. Bhoware, A. P. Singh, J. Mol. Catal. A-Chem. 266 (2007) 118-130.

[58] W. Trakarnpruk, Mendeleev Commun. 26 (2016) 256–258.

[59] C. M. Chanquía, A. L. Cánepa, J. Bazán-Aguirre, K. Sapag, E. Rodríguez-Castellón, P. Reyes, E. R. Herrero, S. G. Casuscelli, G. A. Eimer, Micropor. Mesopor. Mat. 151 (2012) 2–12.

[60] M. V. Landau, S. P. Varkey, M. Herskowits, O. Regev, S. Pezner, T. Sen, Z. Luz, Micropor. Mesopor. Mat. 33 (1999) 149-163.

[61] G. A. Eimer, L. B. Pierella, G. A. Monti, O. A. Anunziata, Catal. Commun. 4 (2003) 118-123.

[62] G. A. Eimer, L. B. Pierella, G. A. Monti, O. A. Anunziata, Catal. Lett. 78 (2002) 65-75.

[63] C. M. Chanquía, A. L. Cánepa, E. L. Winkler, E. Rodríguez-Castellón, S. G. Casuscelli, G. A. Eimer, Mater. Chem. Phys. 175 (2016) 172-179.

[64] Y. Lu, J. Zheng, J. Liu, J. Mu, Micropor. Mesopor. Mat. 106 (2007) 28-34.

[65] V. R. Elías, E. G. Vaschetto, K. Sapag, M. I. Oliva, S. G. Casuscelli, G. A. Eimer, Catal. Today 172 (2011) 58-65

[66] T. Tsoncheva, I. Genova, M. Stoyanova, M. M. Pohl, R. Nickolov, M. Dimitrov, E. Sarcadi-Priboczki, M. Mihaylov, D. Kovacheva, Appl. Catal. B Environ. 147 (2014) 684–697.

[67] N. I. Cuello, V. R. Elías, C. Rodriguez Torres, M. E. Crivello, M. I. Oliva, G. A. Eimer, Micropor. Mesopor. Mat. 203 (2015) 106-115.

[68] S. Shen, J. Chen, R. T. Koodali, Y. Hu, Q. Xiao, J. Zhou, X. Wang, L. Guo, Appl. Catal. B Environ. 150–151 (2014) 138-146.

[69] J. M. Thomas, W. J. Thomas, Principles and Practice of Heterogeneous Catalysis, VCH, New York, 1997.

[70] B. Sun, E. P. Reddy, P. G. Smirniotis, Appl. Catal. B-Environ. 57 (2005) 139–149.

[71] A. L. Cánepa, C. M. Chanquía, G. A. Eimer, S. G. Casuscelli, Appl. Catal. A-Gen. 462– 463 (2013) 8-14.

Figure captions

Figure 1. XRD patterns of the M-M(60) catalysts.

Figure 2. Diffuse reflectance UV−Vis spectra of M-M(60) materials.

Figure 3. Conversion of BzOH and selectivity to BzH versus reaction time over: (♦ ◊)

V-M(60), (■ □) Fe-M(60) and (● ○) Co-M(60). Reaction conditions: $BzOH/H_2O_2$ molar

ratio = 4/1; catalyst = 100 mg, temperature = 70 °C; solvent AcN.

Figure 4. Temperature Program Reduction (TPR) of Fe-M(60) sample.

Figure 5. Diffuse reflectance UV-Vis spectra of Fe modified materials.

Figure 6. TON values of BzOH (◊) and selectivity to reaction products: (▲) BzH, (●)

BzA and (■) BzB as a function of reaction time and $BzOH/H_2O_2$ molar ratio of **(a)** 4/1,

(b) 2/1 and **(c)** 1/1.

Figure 7. Reuse of V-M(60) for BzOH oxidation. Reaction conditions: $BzOH/H_2O_2$

molar ratio = 4/1 with further addition of H_2O_2 at 1 h, temperature = 70 °C, catalyst=

100 mg, reaction time = 7 h.
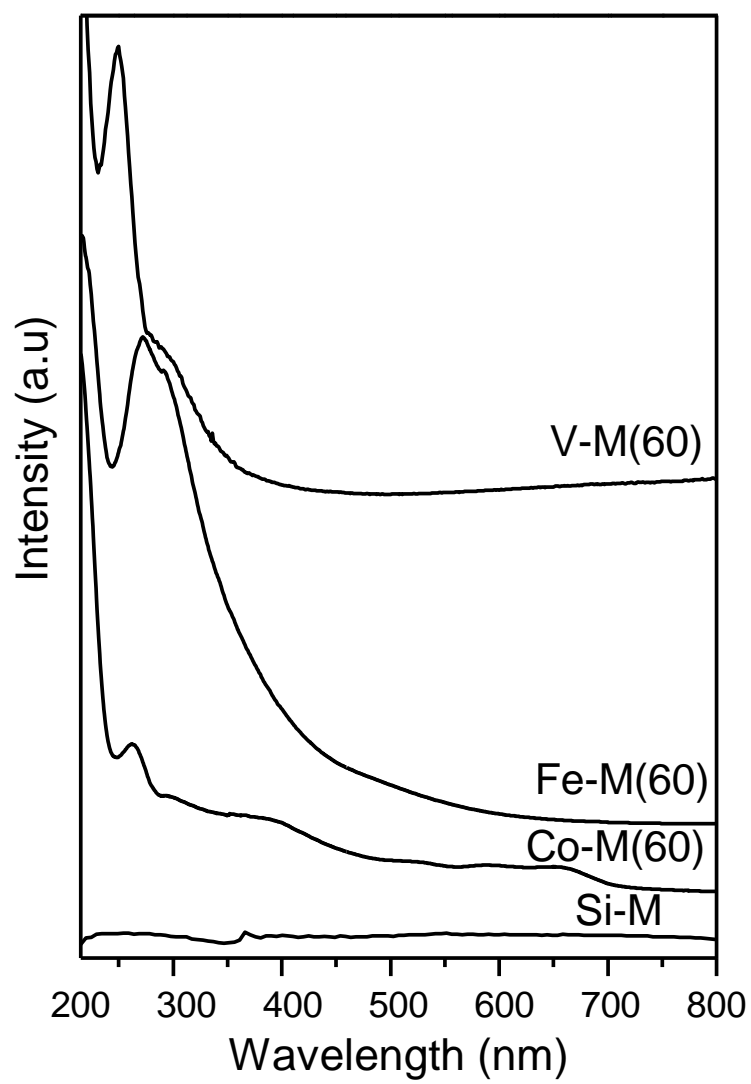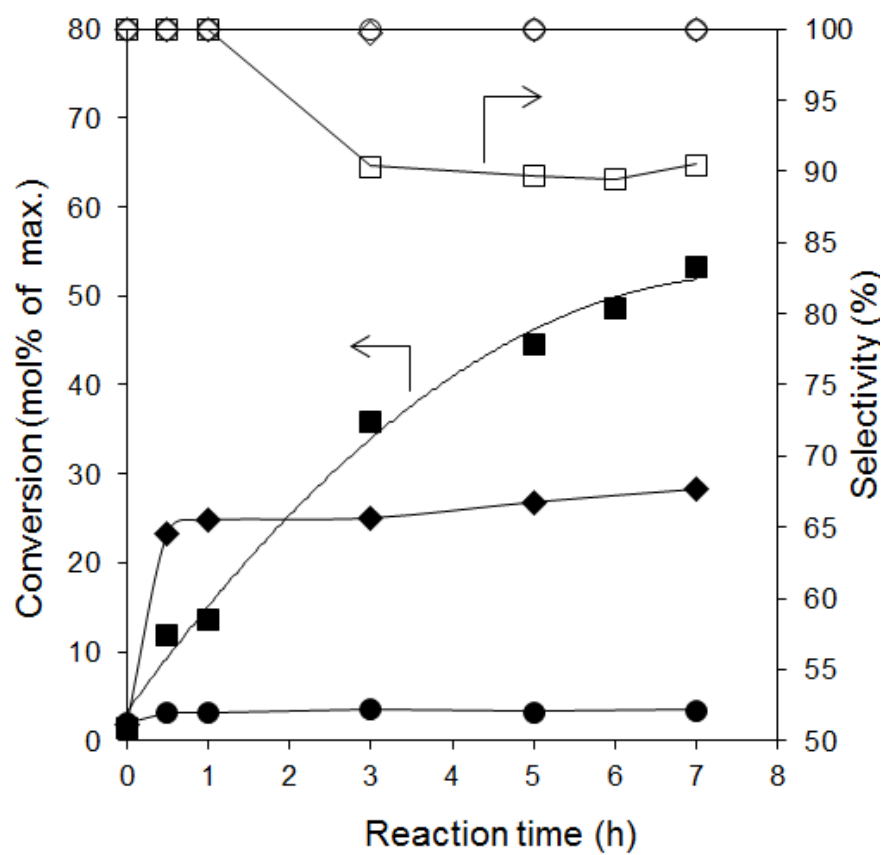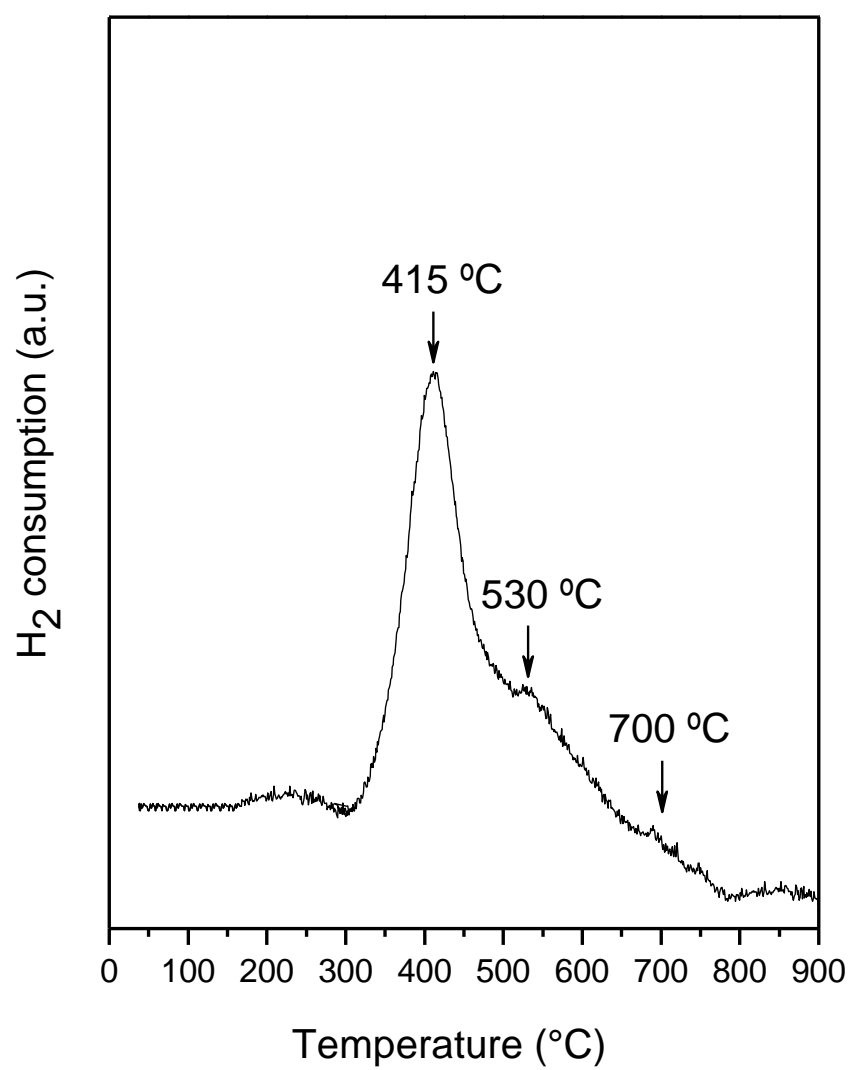
Figure 1.
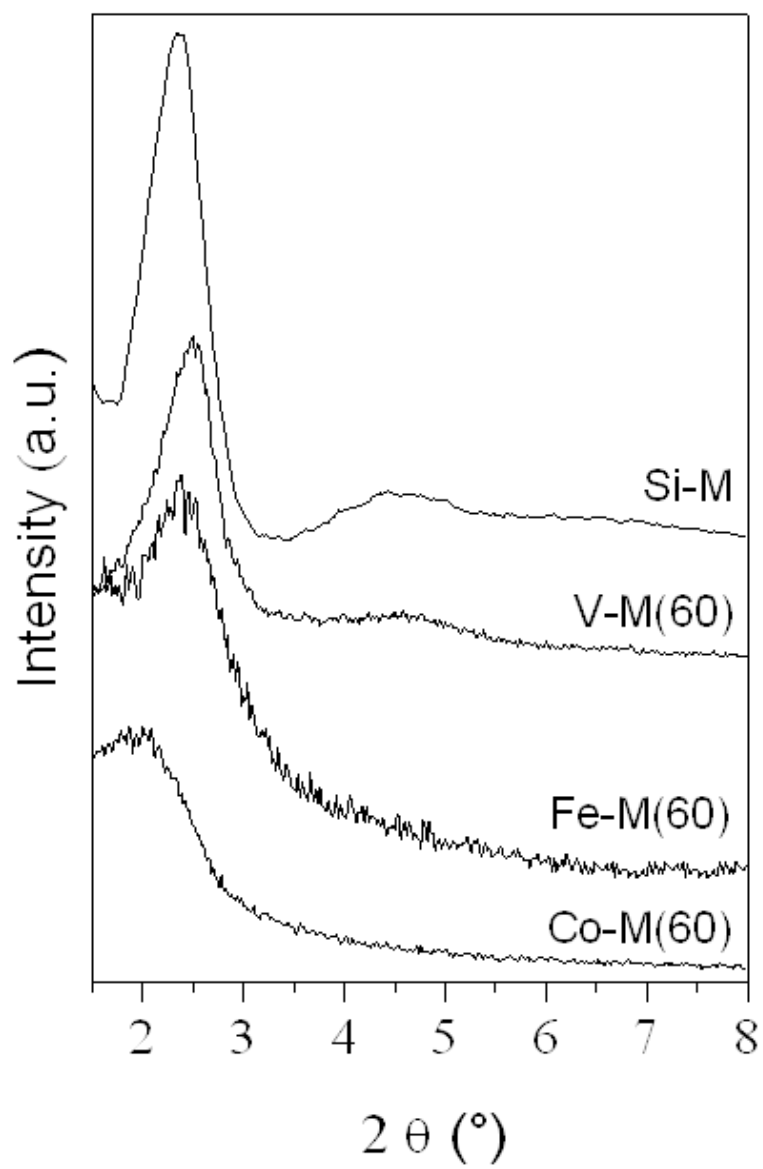
Figure 2.

Figure 3.

Figure 4.

415 ⁰C

530 ⁰C

700 ⁰C

H₂ consumption (a.u.)

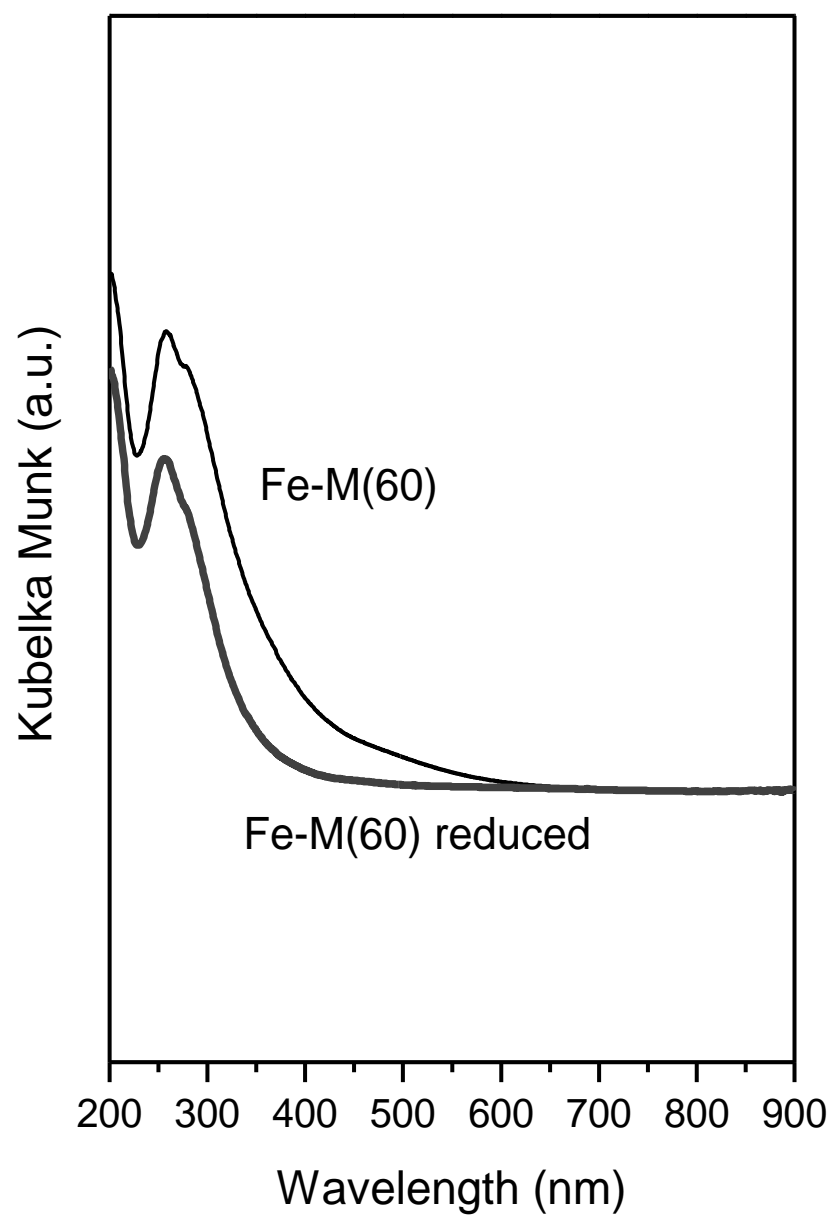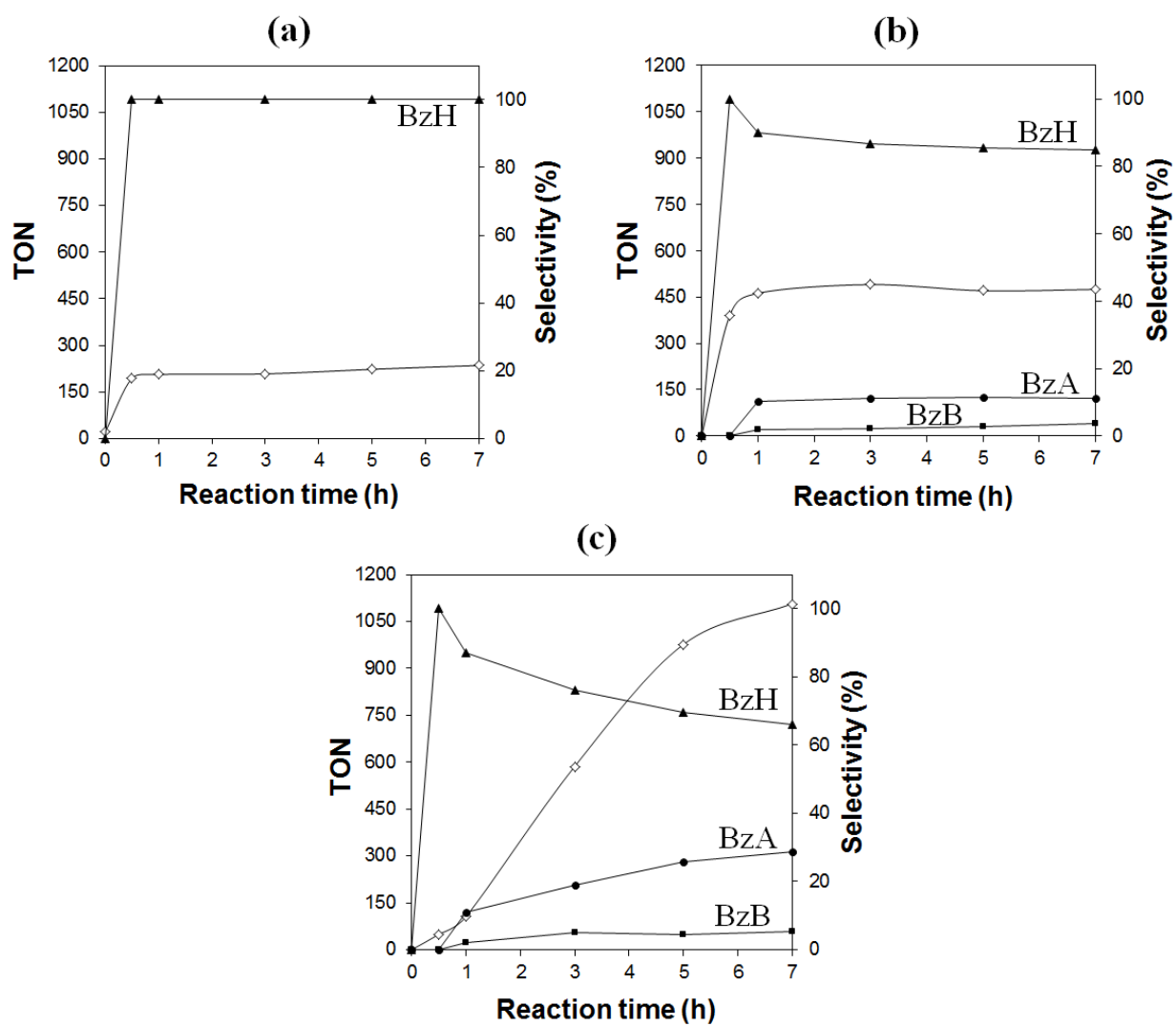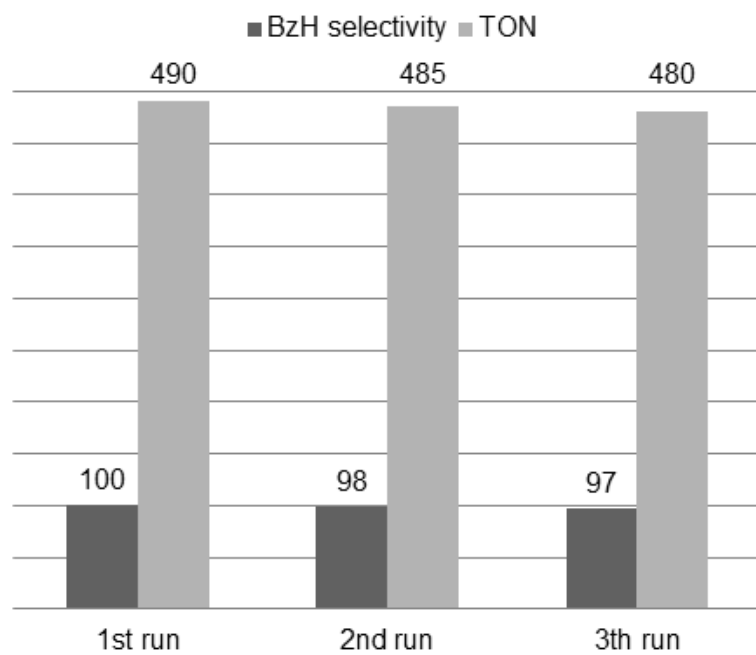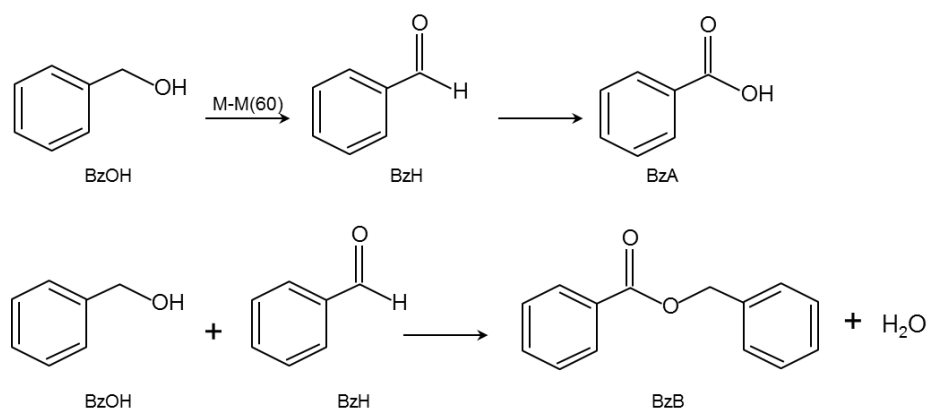Temperature (°C)

Figure 5

Figure 6.

Figure 7.

Scheme 1. Products obtained from benzyl alcohol oxidation employing M-M(60).

Benzaldehyde (BzH), Benzoic acid (BzA), Benzyl benzoate (BzB).

Table 1. Chemical composition and specific surface of the synthesized solids.

Sample	Metal content[a] (wt. %)	A_{BET}[b] ($m^2.g^{-1}$)	a_0[c] (nm)
Si-M	-	1398	4.34
V-M(60)	0.14	1380	4.09
Fe-M(60)	1.34	1370	4.23
Co-M(60)	2.25	468	5.18

[a] In the final solid.

[b] BET specific area

[c] $a_0 = (2/\sqrt{3})d_{100}$

Table 2. BzOH oxidation with H_2O_2 on M-M(x) catalysts under standards conditions.

Sample	BzOH Conversion	Selectivity (%) BzH	BzA	BzB	BzH Yield (%)	TON
V-M(60)	7.1[a] (28.3)[b]	100	-	-	7.1	235.0
Fe-M(60)	13.3[a] (53.2)[b]	90.5	6.0	3.5	12.0	50.5
Co-M(60)	0.9[a] (3.5)[b]	100	-	-	0.9	2.1

Standards conditions: BzOH/H_2O_2 molar ratio = 4/1; catalyst = 100 mg, temperature = 70 °C; solvent AcN, reaction time = 7 h.

[a] BzOH conversion (%)

[b] BzOH conversion (mol % of max.)